Correlation Characteristics-Based Channel Estimation Method for GFDM Systems

Xiaotian Li, Xiaoqing Yan, Zitian Zhao, Jiameng Pei
School of Information Science and Engineering, Hebei University of Science and Technology, Shijiazhuang, China

***Abstract*—Generalized Frequency Division Multiplexing (GFDM) has broad application prospects due to its flexible subcarrier structure and low out-of-band leakage. Traditional channel estimation methods for GFDM systems rely on inserting a large number of pilot sequences, which reduces the data transmission rate. To address this problem, a channel estimation method for GFDM systems based on subcarrier correlation is proposed. First, according to the time–frequency characteristics of the prototype filter in the GFDM system, a pilot sequence with a two-dimensional time–frequency block structure (CTFP) is designed. This sequence is adjusted based on the parameters of the prototype filter. Then, the correlation among subcarriers is utilized for channel estimation, which effectively reduces the pilot overhead and improves the data transmission rate and interference resistance of the system. Simulation results show that under the same total time slot overhead, the mean square error and bit error rate performance of the proposed correlation-based methods are similar to those of existing methods, while the data transmission rate is improved by 14.97% compared with conventional methods.**

***Keywords*—GFDM; channel estimation; correlation; pilot**

I. Introduction

Generalized Frequency Division Multiplexing (GFDM) has been widely used in modern wireless communication systems because of its advantages, such as low out-of-band radiation and high flexibility [1]. As a multicarrier modulation scheme, GFDM is an extension and improvement of the classical Orthogonal Frequency Division Multiplexing (OFDM) technology [2]. Accurate channel parameter estimation is essential for reliable signal detection and demodulation at the receiver of a GFDM system. However, since the GFDM system introduces a prototype filter structure, the subcarriers are no longer strictly orthogonal, and inter-carrier interference affects the accuracy of channel estimation. Therefore, research on channel estimation techniques for GFDM systems is of great significance and practical value [3].

At present, research on channel estimation techniques for GFDM systems mainly focuses on interference suppression and performance improvement. In 2009, G. Fettweis et al. [4] first proposed GFDM as a generalized concept of digital multicarrier transceivers. This system was developed by the Vodafone Chair Mobile Communications Systems team at the Technical University of Dresden in Germany. Tazehkand B. M. et al. [5] proposed a low-complexity successive interference cancellation (SIC) technique for GFDM systems, which mainly solved the self-interference problem in GFDM. The proposed SIC method has three operation modes. Mode 1 eliminates both in-band and adjacent subcarrier interference, mode 2 removes only in-band interference, and mode 3 removes only adjacent subcarrier interference. V. Vincent et al. [6] proposed a threshold-based technique to estimate the channel impulse response (CIR) length from the first samples with a length equal to the cyclic prefix (CP). An adaptive scaling method was designed to reduce the estimation error probability, and a simple signal-to-interference-plus-noise ratio (SINR) estimation method was also proposed to effectively suppress noise and interference. Tai et al. [7] proposed an interference cancellation pilot design scheme, in which interference pre-cancellation was achieved during pilot generation. This method improved the accuracy of LMMSE channel estimation in GFDM and reduced the symbol error rate in high SNR regions. However, the computational complexity increased significantly when the number of subcarriers K became large. N. A. et al. [8] designed an improved Turbo receiver and modified the modulator used for pilot insertion. They proposed an iterative channel estimation algorithm combined with threshold control, which solved the noise enhancement problem that conventional channel estimation methods could not handle in GFDM systems, but the computational complexity remained high. Zhang et al. [9] studied a lattice-reduction-aided signal detection algorithm, which reduced computational complexity but did not consider more complex practical channel conditions. S. Ehsanfar et al. [10] proposed a frequency-domain orthogonal pilot insertion method suitable for highly frequency-selective channels without the need for precoding. This method reduced interference and improved performance, but at the cost of lower spectral efficiency and higher complexity. A. M. Bello et al. [11] proposed a joint synchronization and channel estimation method for GFDM systems, which reduced the estimation error of synchronization and channel estimation, but the computational complexity was high. A. Mohammadian et al. [12] proposed an iterative algorithm for joint channel and phase noise estimation, which solved the problem of joint channel estimation and phase noise compensation in GFDM systems and reduced complexity, but lacked analysis for time-varying channels in high mobility scenarios. Liu et al. [13] proposed a subspace-based blind initial channel estimation method, which jointly estimated the channel and carrier frequency offset (CFO), but the computational complexity was high. J. Inga et al. [14] proposed a PAPR reduction technique and a pilot-assisted channel estimation method, which improved system performance but lacked validation under complex channel conditions. Wang et al. [15] proposed an estimation method based on the correlation between preamble symbols and middle symbols, where the carrier frequency offset was estimated using a mean estimation method. However, this method was

not verified under complex environments such as multipath fading. J. Jeong et al. [16] proposed a GFDM system based on eigen decomposition, aiming to eliminate inherent system interference and achieve interference-free pilot insertion, but it required heavy computation. Shayanfar H. et al. [17] addressed the problems of limited estimation range and high computational complexity, and proposed a joint CFO and channel estimation algorithm based on the maximum likelihood criterion, but it did not consider fast time-varying channels. Ehsanfar S. et al. [18] studied pilot-based channel estimation in GFDM systems and compared the least squares, harmonic mean, and linear minimum mean square error (LMMSE) estimation methods. However, they did not consider fast time-varying channels, and the complexity was still high. Anish Pon Yamini K. et al. [19] proposed a pilot-based channel estimation scheme using least squares and LMMSE estimators. They focused on the impact of pilot pattern design on estimation performance, but the spectral efficiency was poor and the data transmission rate was low. Moreover, the time-frequency characteristics of the GFDM prototype filter are not fully utilized, and the correlation between subcarriers is not considered.

In summary, blind estimation methods do not require pilot insertion but have low estimation accuracy, while pilot-based methods achieve higher accuracy but require many pilot symbols, leading to a lower data transmission rate. Moreover, existing methods do not fully exploit the time-frequency characteristics of the GFDM prototype filter. When considering the correlation among subcarriers, these methods only focus on the frequency waveform correlation and do not take the terminal geographic location in practical scenarios into account. Therefore, there is still room for further optimization of pilot overhead and time slot allocation in GFDM channel estimation. Based on the above studies, this study proposes a channel estimation method for GFDM systems based on the correlation between subcarriers. The main contributions of this study are summarized as follows:

- We design a pilot sequence with a two-dimensional time–frequency block structure, named Composite Time-Frequency Pilot (CTFP), based on the time–frequency characteristics of the prototype filter in the GFDM system. In the time domain, the amplitude of the pilot is adjusted according to the parameters of the prototype filter, while in the frequency domain, different subcarriers are distinguished by unique phase encoding. This design makes the pilots approximately orthogonal or complementary in the non-orthogonal time–frequency structure of GFDM. This reduces the inherent interference between pilots and between pilots and data, addressing the gap in exploiting the filter characteristics to mitigate interference.
- By analyzing the time-domain response characteristics of the prototype pulse filter, the energy weighting coefficient of pilot symbols at different time slots is dynamically calculated, which realizes non-uniform power allocation of pilots in the time domain.
- A channel estimation method based on correlation characteristics is proposed to solve the problem of low data transmission rate. Under certain channel conditions, subcarriers are grouped according to their correlation. Only one pilot is inserted in each group for estimation, and other subcarriers in the same group share the same channel estimation value. The time slots without pilots are used to transmit data symbols. It improves the data transmission rate, filling the gap in data rate enhancement.

The rest of this study is organized as follows: Section II describes the basic model of the GFDM system, including the modulation and demodulation principles and the implementation of the prototype filter. Section III presents the pilot design and channel estimation method. Section IV provides the simulation results and analysis. Section V presents a discussion on a channel estimation method for GFDM systems based on correlation characteristics. Finally, Section VI concludes this study.

II. GFDM System Model

A. GFDM Basic Model

A GFDM system with K subcarriers and M subsymbols has $N = K \times M$ grid points in the two-dimensional time–frequency plane. Each grid point carries a complex data symbol obtained through Quadrature Amplitude Modulation (QAM) mapping. The block diagram of channel estimation for the GFDM system is shown in Fig. 1. The N complex data symbols are represented as a vector [see Eq. (1)]:

$$d = \left[d_{0,0} \dots d_{\{K-1,0\}} d_{0,1} \dots d_{\{K-1,M-1\}}\right]^T \quad (1)$$

where, $d_{k,m}$ denotes the data symbol transmitted on the K -th subcarrier of the M -th subsymbol, and the data symbols are assumed to be independent and identically distributed. The transmitted signal of the GFDM system can be expressed as Eq. (2):

$$x[n] = \sum_{k=0}^{K-1} \sum_{m=0}^{M-1} d_{k,m} \times g_{k,m}[n] \quad (2)$$

where, $d_{k,m}$ represents the data transmitted on the k -th subcarrier and the m -th time symbol, and $g_{k,m}[n]$ denotes the time–frequency shifted filter corresponding to the indices k and m.

B. Principle of GFDM Modulation and Demodulation

As a multicarrier modulation technique, Generalized Frequency Division Multiplexing (GFDM) maps data symbols onto multiple subcarriers and subsymbols. The prototype filter is used for pulse shaping to achieve efficient data transmission. The GFDM modulation process can be expressed in matrix form. The time-domain transmitted signal is represented as a vector [see Eq. (3)]:

$$x = \left[x[0]x[1] \dots x[N-1]\right]^T \quad (3)$$

Then, the GFDM modulation process can be expressed as Eq. (4):

$$x = Ad \quad (4)$$

where, A is the $N \times N$ GFDM modulation matrix, which is defined as Eq. (5):

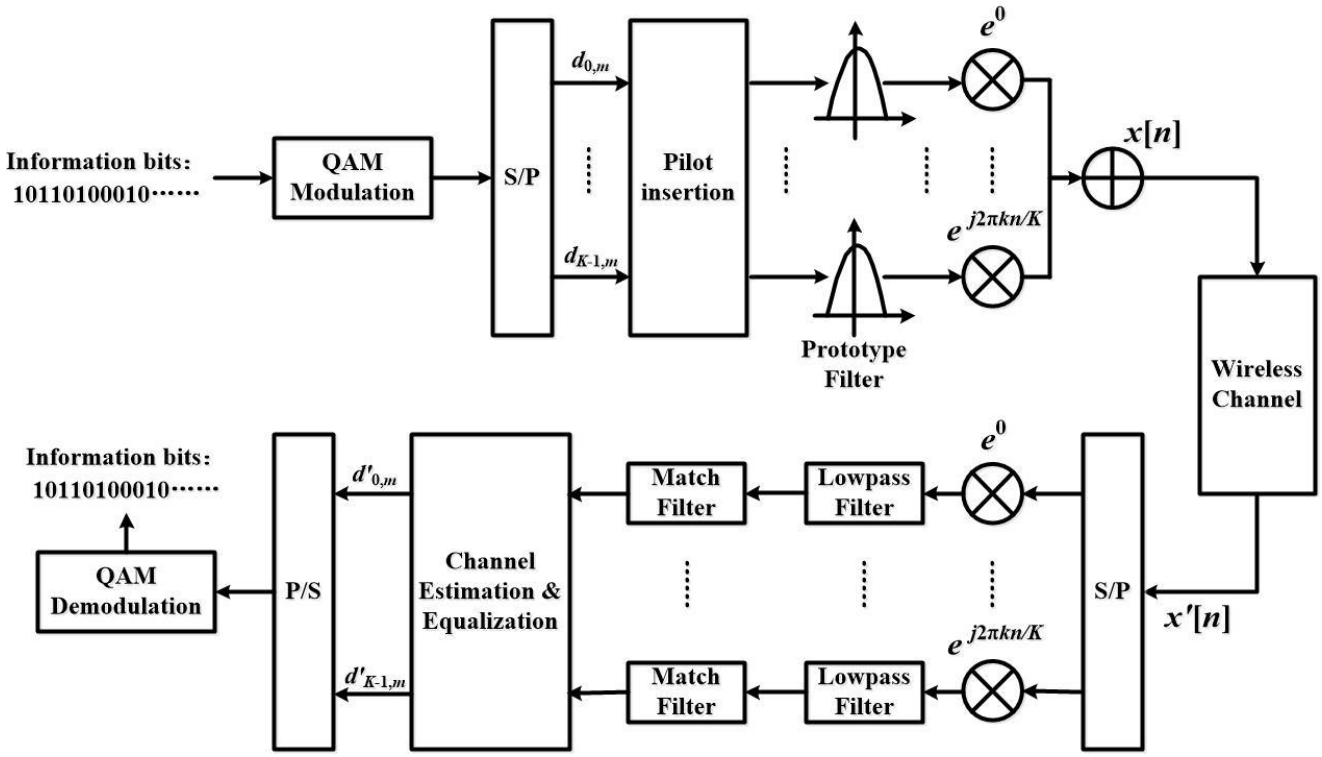

Fig. 1. Information transmission block diagram of the GFDM system.

$$A = \left[g_{\{0,0\}}g_{\{1,0\}} \cdots g_{\{K-1,0\}}g_{\{1,0\}} \cdots g_{\{K-1,M-1\}}\right] \quad (5)$$

Among them, $g_{k,m} = [g_{k,m}[0]g_{k,m}[1] \ldots g_{k,m}[N-1]]^T$ is a column vector with a length of N. The modulation on each subcarrier is expressed as follows [see Eq. (6)]:

$$x[n] = \sum_{k=0}^{K-1}\sum_{m=0}^{M-1} d_{k,m} \times g[(n-mK)modN]e^{\left\{j\left(\frac{2\pi}{K}\right)kn\right\}} \quad (6)$$

Expanding the above expression, we obtain Eq. (7):

$$x = \sum_{k=0}^{K-1}\sum_{m=0}^{M-1} d_{k,m} \times g_{k,m} \quad (7)$$

In the GFDM system, the time shift is performed in a periodic manner, and the frequency shift is carried out according to the following equation, forming a frequency shift vector [see Eq. (8)]:

$$f_k[n] = e^{j2\pi\frac{k}{K}n} \quad (8)$$

C. Design of Pulse Shaping Filter

An important difference between GFDM and OFDM lies in the prototype filter used for the subcarriers. OFDM employs a rectangular pulse filter, while GFDM uses a non-rectangular pulse filter. The pulse shaping function is given as follows [see Eq. (9)]:

$$g_{\{k,m\}[n]} = g_{m[n]e^{j\left(\frac{2\pi}{K}\right)kn}} = g[(n-mK)_N]e^{j\left(\frac{2\pi}{K}\right)kn} \quad (9)$$

Here,$(\cdot)_N$ denotes the modulo-N operation,$g[n]$ represents the prototype filter, and $g_m[n]$ is the pulse shaping filter for the m-th subsymbol. In this work, the Root Raised Cosine (RRC) filter is used. The time-domain expression of the Root Raised Cosine filter is given as follows [see Eq. (10)]:

$$g(t) = \begin{cases} \frac{1}{T}\left(1+\beta\left(\frac{4}{\pi}-1\right)\right), t=0 \\ \frac{\beta}{T\sqrt{2}}\left[\left(1+\frac{2}{\pi}\right)sin\left(\frac{\pi}{4\beta}\right)+\left(1-\frac{2}{\pi}\right)cos\left(\frac{\pi}{4\beta}\right)\right], t=\pm\frac{T}{4\beta} \\ \frac{sin\left(\frac{\pi t(1-\beta)}{T}\right)+\frac{4\beta t}{T}\cdot cos\left(\frac{\pi t(1+\beta)}{T}\right)}{\pi t\left[1-\left(\frac{4\beta t}{T}\right)^2\right]}, otherwise \end{cases} \quad (10)$$

Here, $T$is the symbol period, $\beta$is the roll-off factor, and $t$is the time variable.

In the GFDM system, there is significant overlap between subcarriers and symbols in the time and frequency domains. The rectangular pulse used in traditional OFDM causes considerable spectral leakage. By applying the RRC filter to shape each subcarrier, better frequency localization can be achieved, adjacent channel interference can be reduced, and asynchronous transmission can be supported. Secondly, the structure of the time-frequency transform filter is given as follows [see Eq. (11)]:

$$g_{k,m}[n] = g[(n-mk)modN] \cdot e^{j2\pi\frac{k}{K}n} \quad (11)$$

Here, $g[n]$ denotes the prototype filter; mK represents the time shift, since there are K samples between every M symbol intervals; $e^{j2\pi\frac{k}{K}n}$ denotes the frequency shift used for subcarrier multiplexing; and $N = KM$ represents the total symbol length.

III. Channel Estimation Method

A. Least Squares Estimation

The Least Squares (LS) estimation algorithm is a basic method used for data fitting and parameter estimation. Its main idea is to find the optimal model parameters by minimizing the sum of squared errors between the observed data and the model-predicted values. In the estimation process, each subcarrier k is fitted individually using the LS method, and the result is obtained as follows [see Eq. (12)]:

$$\hat{h}_k^{LS} = argmin\left|r_{k,1} - p\hat{h}\right|^2 \quad (12)$$

Here, $\hat{h}_k^{LS}$ denotes the LS channel estimate on the k-th subcarrier. k is the subcarrier index, representing the k-th subcarrier in the frequency domain. $r_{k,1}$ is the received signal at the receiver on the k-th subcarrier and the first pilot symbol. p represents the known pilot symbol. $\hat{h}$ denotes the channel coefficient to be estimated.

Ordinary least squares analysis of the observational data yields Eq. (13):

$$\hat{h}_k^{LS} = \frac{p*r_{k,1}}{|p|^2} \quad (13)$$

Here, $p*$denotes the complex conjugate of the pilot symbol p. $|p|^2$ denotes the power of the pilot symbol.

This method uses unit power, which can be simplified to Eq. (14):

$$\hat{h}_k^{(LS)} = \frac{r_{k,1}}{p} \quad (14)$$

Here, (p) represents the pilot symbol.

B. Design of a Two-Dimensional Time-Frequency Block-Based Pilot Structure

In GFDM systems, there is incomplete orthogonality between subcarriers and between time slots. The use of RRC filters causes both inter-subcarrier interference and inter-symbol interference. Therefore, conventional pilot designs are no longer optimal, as they are affected by leakage from neighboring symbols and interference from adjacent subcarriers. To address these issues, a pilot structure is designed in the two-dimensional time-frequency domain. Compared with conventional pilots, the proposed design maintains approximate orthogonality or complementarity in the non-orthogonal time-frequency domain of GFDM, which enhances interference resistance and improves estimation accuracy.

The key of the GFDM system lies in the fact that each "subsymbol-subcarrier" block is obtained by time-shifting and frequency-shifting a prototype pulse filter, resulting in overlapping in both time and frequency domains. Here, the pulses are non-rectangular and not strictly orthogonal. A two-dimensional time-frequency block-based pilot structure, named Composite Time-Frequency Pilot (CTFP), is designed. The CTFP is a composite sequence distributed over multiple time slots on the same subcarrier, weighted by the prototype pulse, and phase-coded within the subcarrier. This pilot structure distinguishes different subcarriers in the frequency domain, with each subcarrier having a unique phase code. In the time domain, the energy is distributed using the GFDM shaping filter (RRC pulse shaping), ensuring that the pilot symbols have the same time-domain characteristics as the data symbols.

In GFDM, the length of each data block is $N = K \cdot M$, where K is the number of subcarriers and M is the number of subsymbols. First, a QPSK pilot symbol is defined as Eq. (15):

$$s_p = \frac{1+j}{\sqrt{2}} \quad (15)$$

Here, s_p is the pilot symbol modulated using QPSK. j denotes the imaginary unit, where $j = \sqrt{-1}$.

In a conventional GFDM system, the pilot symbol for each subcarrier is usually given by Eq. (16):

$$p_{trad} = s_p \quad (16)$$

Here, p_{trad} denotes the pilot symbol in the conventional GFDM system.

Each pilot subcarrier transmits only one complex constant in one time slot, and the pilot power is concentrated at one time-frequency position.

The pilot vector is constructed using the time-domain response of the RRC filter, which reflects the energy of the filter's power distribution in this time slot [see Eq. (17)].

$$w_{CTFP}[m] = \sum_{n=0}^{L-1} |g[(n-(m-1)K) mod L]|^2 \quad (17)$$

Here, $w_{CTFP}[m]$denotes the energy weighting of the CTFP pilot at the m-th time slot. $g[\cdot]$ denotes the time-domain impulse response of the RRC filter. L denotes the filter length or the GFDM block length. m denotes the subsymbol index.

Energy equalization is performed so that the total energy of CTFP pilots is the same as that of traditional pilots for comparison [see Eq. (18)].

$$\alpha = \sqrt{\frac{E_{trad}}{E_{CTFP}}} = \sqrt{\frac{|s_p|^2}{|s_p|^2 \cdot \|w\|^2}} \quad (18)$$

Here, α denotes the energy normalization factor. E_{trad} denotes the total energy of the traditional pilot. E_{CTFP} denotes the total energy of the CTFP pilot. $\|w\|^2$ denotes the energy norm of the weighting vector w_{CTFP}.

Second, a complex exponential phase code is assigned to each subcarrier, yielding Eq. (19):

$$c_k = e^{j\frac{2\pi k}{K}} \quad (19)$$

where, $k = 0, 1, \ldots, K-1$, so that pilots of different subcarriers can be distinguished in the frequency domain.

At the transmitter, the CTFP pilot is constructed, yielding Eq. (20):

$$P_k = s_p \cdot c_k \cdot \alpha w \quad (20)$$

where, s_p denotes the pilot symbol.

Thus, each pilot has time-domain spreading and frequency-domain distinction, a two-dimensional block pilot structure [see Eq. (21)]:

$$CTFP_{pilot} = \underbrace{(time-shaping)}_{w_{CTFP}\alpha} \otimes \underbrace{(freq-phase\ coding)}_{c_k} \quad (21)$$

It is distributed in the time slot of this subcarrier. The amplitude diagram and phase diagram of the pilot internal structure are shown in Fig. 2 and Fig. 3.

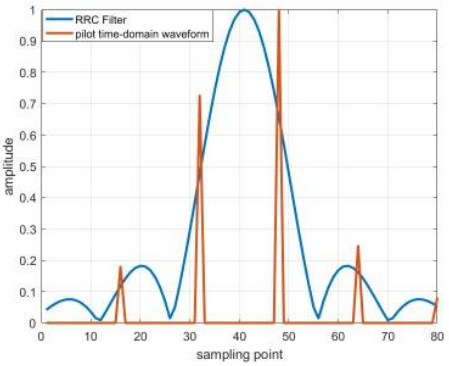

Fig. 2. Comparison of pilot amplitude values and filter waveform.

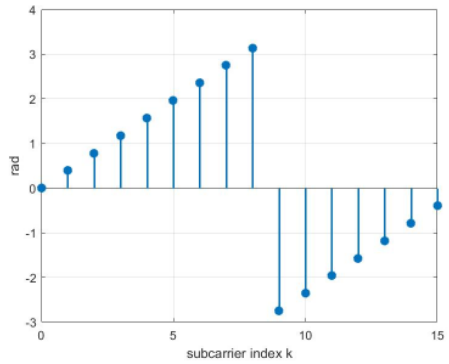

Fig. 3. Variation of the pilot phase.

C. Channel Estimation Method Based on Correlation

To improve the transmission efficiency of channel estimation in the GFDM system and give full play to the great advantages of CTFP in the GFDM system, a channel estimation method based on correlation is proposed on the basis of the traditional Least Squares (LS) estimation. This method is based on the fact that under relatively flat channel conditions, the frequency-domain channel response usually shows strong correlation, so the channel gains of adjacent subcarriers can be regarded as highly correlated. Based on this characteristic, the correlation method reduces the impact of channel estimation error of a single subcarrier by introducing the concept of a subcarrier group. Specifically, the system first performs LS estimation on each subcarrier at the position where CTFP is inserted to obtain the initial channel estimation value. Then, for the k-th subcarrier, its final channel estimation is not directly taken from its own estimation result, but replaced by the estimation result of the reference subcarrier in its corresponding correlated subcarrier group. For example, among subcarriers 1–4, all subcarriers use the estimation value of subcarrier 1 as the channel estimation. Among subcarriers 5–8, the channel estimation value of subcarrier 5 is uniformly adopted, and so on. In this way, while reducing pilot overhead, the system allows time slots without pilot configuration to be used for data transmission, thus utilizing spectrum resources more efficiently and improving the proportion of effective data transmission to a certain extent.

Divide K subcarriers into several groups. In this method, each group has a length of 4. Channel estimation is performed only on the first subcarrier of each group, and the other subcarriers adopt the estimation result of the first subcarrier, that is, use it directly, as shown in Fig. 4.

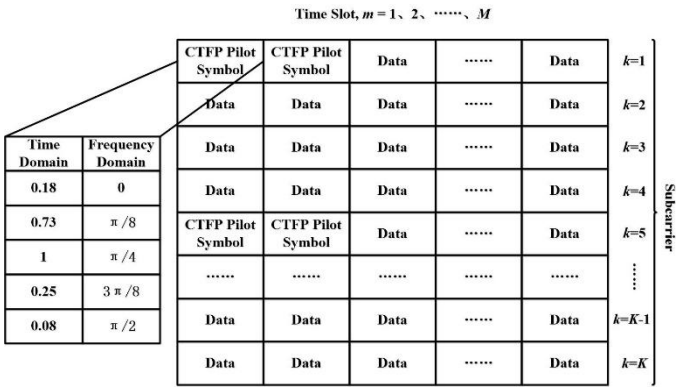

Fig. 4. The CTFP pilot insertion in the GFDM system.

The data block transmitted in a GFDM system is composed of K subcarriers and M subsymbols. Its time frequency structure is characterized by K subcarriers in the frequency domain and M subsymbols in the time domain. The correlation among subcarriers is used by considering the cross-correlation function in the frequency domain. The EPA model in the 3GPP LTE channel model, which refers to the Extended Pedestrian A model, is applied. This model is used for low-speed movement, such as pedestrians in typical indoor or micro cell environments.

The time-domain random multipath channel is represented by the impulse response $h(\tau)$, where τ is the delay. The power delay profile [Power Delay Profile (PDP)] is given as Eq. (22):

$$P(\tau) = \mathbb{E}[|\, h(\tau)\,|^2] \quad (22)$$

The frequency domain channel frequency response is Eq. (23):

$$H(f) = \int_{-\infty}^{\infty} h(\tau) e^{-j2\pi f\tau} d\tau \quad (23)$$

The cross correlation at two different frequencies f_1 and f_2 is expressed as Eq. (24):

$$R_H(f_1, f_2) \triangleq \mathbb{E}[H(f_1)H^*(f_2)] \quad (24)$$

By substituting the definition of $H(f)$ and using the stationarity assumption, that is, the delay components in the time domain are uncorrelated and $E[h(\tau)h^*(\tau')] = 0$ when $\tau \neq \tau'$, and equal to $P(\tau)$ when $\tau = \tau'$, we can obtain Eq. (25):

$$R_H(f_1, f_2) = \int_{-\infty}^{\infty} P(\tau) e^{-j2\pi(f_1-f_2)\tau} d\tau \quad (25)$$

Let the frequency difference be $\Delta f = f_1 - f_2$ .Then the autocorrelation function only depends on Δf [see Eq. (26)]:

$$R_H(\Delta f) = \int_{-\infty}^{\infty} P(\tau) e^{-j2\pi(f_1-f_2)\tau} d\tau \quad (26)$$

The normalized correlation coefficient, which gives the correlation between the two frequency points, is complex-valued. By applying the Fourier transform to the PDP, it is expressed as Eq. (27):

$$\rho(\Delta f) = \frac{R_H(\Delta f)}{R_H(0)} = \frac{\int P(\tau) e^{-j2\pi\Delta f\tau} d\tau}{\int P(\tau) d\tau} \quad (27)$$

The magnitude $|\rho(\Delta f)| \in [0,1]$ describes the strength of the correlation between the frequencies. When $|\rho|$ is close to 1, the frequency domain response is highly correlated under this frequency offset.

If the PDP is a set of discrete multipath components as in the EPA model, the explicit expression of the discrete taps is Eq. (28):

$$P(\tau) = \sum_{n=0}^{N-1} p_n \delta(\tau - \tau_n), p_n \geq 0 \quad (28)$$

We obtain Eq. (29):

$$\rho(\Delta f) = \frac{\sum_{n=0}^{N-1} p_n e^{-j2\pi\Delta f\tau_n}}{\sum_{n=0}^{N-1} p_n} \quad (29)$$

According to Eq. (30):

$$\Delta f = m\Delta f_{\mathrm{sc}} \quad (30)$$

Here, m is the subcarrier index difference, and Δf_{sc} is the subcarrier spacing.

We obtain Eq. (31):

$$\rho(m) = \frac{\sum_n p_n e^{-j2\pi m\Delta f_{\mathrm{sc}}\tau_n}}{\sum_n p_n} \quad (31)$$

When $\omega = 2\pi\Delta f$ is small, the characteristic function can be approximated using a Taylor series expansion [see Eq. (32)]:

$$\rho(\Delta f) = \mathbb{E}[e^{-j\omega\tau}] \approx 1 - j\omega\mu_\tau - \frac{\omega^2}{2}\mathbb{E}[\tau^2] + O(\omega^3) \quad (32)$$

Here, $\mu_\tau = E[\tau]$. Then Eq. (33):

$$|\rho(\Delta f)|^2 \approx 1 - \omega^2 \mathrm{Var}(\tau) + O(\omega^3) \quad (33)$$

By taking the second-order approximation, we obtain Eq. (34):

$$|\rho(\Delta f)| \approx \sqrt{1 - \omega^2 \mathrm{Var}(\tau)} \approx 1 - \frac{\omega^2 \mathrm{Var}(\tau)}{2} \quad (34)$$

Therefore, to require $|\rho| > 0.9$, that is, the magnitude greater than 0.9, the approximate condition is Eq. (35):

$$1 - \frac{\omega^2 \mathrm{Var}(\tau)}{2} > 0.9 \Rightarrow \omega^2 \mathrm{Var}(\tau) < 0.2 \quad (35)$$

By substituting $= 2\pi\Delta f$, we obtain Eq. (36):

$$\Delta f < \frac{1}{2\pi}\sqrt{\frac{0.2}{\mathrm{Var}(\tau)}} \quad (36)$$

Here, $\mathrm{Var}(\tau)$ is the delay variance of the PDP.

By substituting the above values, it can be seen that for $0 \leq \Delta f \leq 2$ MHz, the correlation between subcarriers is always greater than 0.9. This indicates that under the EPA channel conditions, the frequency domain correlation is always higher than 0.9, and channel estimation methods based on correlation characteristics have practical application value.

In spatially correlated channels, under the GFDM framework, the channel responses of two users in the time frequency domain, denoted as $h_1(t,f)$ and $h_2(t,f)$, exhibit spatial correlation. The cross-correlation function between them can be defined as Eq. (37):

$$R_{h_1h_2}(\Delta t, \Delta f) = \mathbb{E}[h_1(t,f)h_2^*(t-\Delta t, f-\Delta f)] \quad (37)$$

Since the support set Ω is the same, that is, $\Delta t \approx 0, \Delta f \approx 0$. By processing the above definition and performing normalization, the expression can be rewritten as shown in Eq. (38):

$$\rho(d) = \frac{\mathbb{E}[\iint_\Omega h_1(t,f)h_2^*(t,f)dtdf]}{\sqrt{\mathbb{E}[|h_1|^2]\mathbb{E}[|h_2|^2]}} \quad (38)$$

Because the support set Ω is identical, the double integral in the above equation can be simplified to a summation over the same set of propagation paths, as given in Eq. (39):

$$\rho(d) = \frac{\mathbb{E}\left[\sum_{p=1}^{P} h_{1,p}h_{2,p}^*\right]}{\sqrt{\mathbb{E}[\sum_p |h_{1,p}|^2]\mathbb{E}[\sum_p |h_{2,p}|^2]}} \quad (39)$$

Assuming that different propagation paths are uncorrelated with each other and that the power of each path is normalized, the above expression can be further simplified as Eq. (40):

$$\rho(d) = \frac{1}{P}\sum_{p=1}^{P} \rho_p(d) \quad (40)$$

where, $\rho_p(d) = \mathbb{E}[h_{1,p}h_{2,p}^*]$ denotes the spatial correlation coefficient of the complex gain on the p-th path.Assume that there are many scattering components arriving at the receiver from different angles θ, and the angular distribution of these components is given by $p(\theta)$. Then, for the two user case, the correlation of the channel complex gains can be described by the classical Clarke model as Eq. (41):

$$\rho_p(d) = \int_{-\pi}^{\pi} P(\theta) e^{-j\frac{2\pi d}{\lambda}\sin\theta} d\theta \quad (41)$$

where, λ is the wavelength and d represents the distance between the two users.Assume that the angles of arrival follow a Gaussian distribution with mean $\theta_0$and standard deviation σ_θ. The corresponding angular power spectrum is given in Eq. (42):

$$p(\theta) = \frac{1}{\sqrt{2\pi}\sigma_\theta}\exp\left(-\frac{(\theta-\theta_0)^2}{2\sigma_\theta^2}\right) \quad (42)$$

Based on the above spatial correlation analysis, under the EPA channel model, when the distance between communication terminals is small, the spatial correlation coefficient of the channel can reach 0.9 or even higher.

Perform channel estimation on the first subcarrier of each group [see Eq. (43)]:

$$\hat{h}_k = \frac{P_k^H r_k}{\|P_k\|^2} \tag{43}$$

Then, directly use the estimated values for other subcarriers [see Eq. (44)]:

$$\hat{h}_k = \hat{h}_{ref} \tag{44}$$

IV. Simulation Experiments and Analysis

A. Experimental Conditions

To evaluate the performance of the proposed correlation-based channel estimation method, Monte Carlo simulations were conducted using MATLAB software. The main parameter settings are presented in Table I.

TABLE I. Parameter Settings

Parameters	Values
Number of subcarriers, K	16、100
Number of subsymbols, M	5、8、100
Modulation scheme	QPSK
Filter	Root-Raised Cosine（RRC）
Filter roll-off factor	0.3
Channel model	AWGN channel
Pilot symbols	QPSK unit power symbol $\frac{1+j}{\sqrt{2}}$
Pilot spacingΔ	2、4、6、8
SNR range	0-30 dB with a step of 5 dB
Number of Monte Carlo Simulations	1000

In the simulation figure, the x-axis represents the signal-to-noise ratio (SNR), and the y-axis represents the mean square error (MSE), which can reflect the accuracy of channel estimation and is defined as Eq. (45):

$$MSE = \frac{1}{K}\sum_{k=0}^{K-1}\left|\widehat{h_k} - h_k\right|^2 \tag{45}$$

B. Information Rate Analysis

It is assumed that the channel is a flat Rayleigh fading channel, in which the channel coefficient within one GFDM block is a complex constant h that does not change with time or frequency. The receiver is affected only by additive white Gaussian noise. Under this assumption, the correlation between subcarriers remains higher than 0.9, which allows the study of the impact of different pilot structures on the data rate. The total number of symbols, that is, the product of time slots and subcarriers, is defined as Eq. (46):

$$N_{tot} = K \cdot M \tag{46}$$

If pilots occupy N_pilot symbols, the number of symbols available for data is Eq. (47):

$$N_{data} = N_{tot} - N_{pilot} \tag{47}$$

Each symbol carries b = $\log_2$ (modulation order) bits, and the information rate is Eq. (48):

$$R = \frac{N_{data}}{N_{tot}} b \tag{48}$$

The unit is bit/s/Hz/subcarrier.

For existing methods, we obtain Eq. (49):

$$N_{pilot} = K \tag{49}$$

For the correlation-based method, with a spacing of s, we can obtain Eq. (50):

$$N_{pilot} = \frac{K}{s} \tag{50}$$

As shown in Fig. 5 and Fig. 6, these figures present a comparison of the information rate between the existing method and the correlation-based method with pilots placed at different subcarrier spacings. Assuming a sampling rate of 1 MHz and a duration of 0.016 ms per time slot, it can be seen from the figures that the information rate gradually increases with the growth of the number of time slots (M) in the GFDM system. Compared with the existing method, the transmission rate of the correlation-based method is higher. This is because the first time slot of each subcarrier in the existing method is occupied by pilots, leading to low spectrum efficiency. As M increases, the pilot ratio gradually decreases, and the rate increases accordingly. The information transmission performance is improved by about 14.97% compared with the existing method when the time slot width is 0.096 ms, about 10.74% when the time slot width is 0.128 ms, and about 2.59% when the time slot width is 0.48 ms. For the correlation-based estimation method, only one pilot is allocated to each group of subcarriers, so the pilot overhead is much lower than that of the existing method. Thus, its rate is significantly higher under all time slot conditions. This result indicates that the correlation-based method has more advantages in terms of the system's information transmission rate.

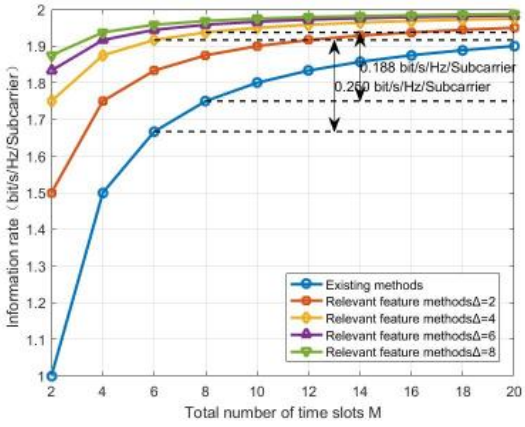

Fig. 5. Comparison of information rate in the GFDM system (K=16).

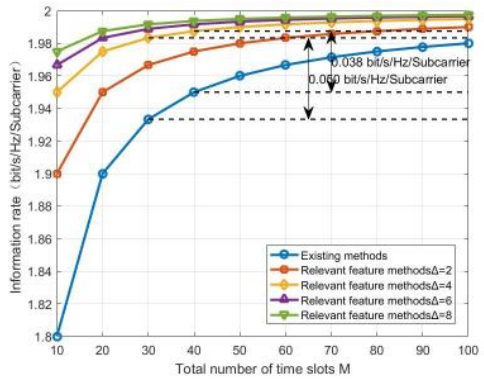

Fig. 6. Comparison of information rate in GFDM system 2 (K=100).

C. Channel Estimation Mean Square Error Performance Analysis

As shown in Fig. 7, the mean square error (MSE) of both the existing method and the correlation-based method decreases with the increase of signal-to-noise ratio (SNR). In terms of channel estimation methods, the existing method has better MSE performance. This is because the correlation-based method uses grouped references, which reduces the number of pilots. Adjacent subcarriers use the same channel estimation result, leading to accuracy loss. In terms of pilot design, it can be clearly seen that the CTFP pilot design has stronger anti-interference capability and better MSE performance. This is because the pilot design combines the characteristics of the time-frequency domain and the prototype filter, improving anti-interference capability. Thus, it can be concluded that the existing method is better in estimation accuracy, while the correlation-based method is more suitable for use under low overhead requirements. Moreover, the CTFP pilot structure has better performance than the traditional pilot structure.

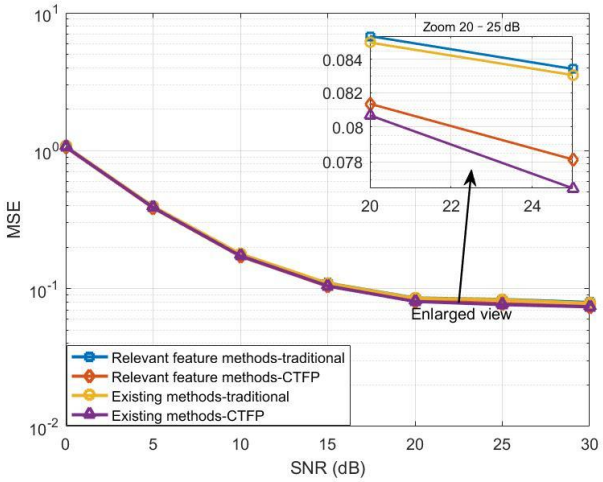

Fig. 7. Comparison of MSE in the GFDM system.

As shown in Fig. 8, the impact of inter-subcarrier channel correlation on the correlation-based method is analyzed. When $\alpha = 0$ (i.e., inter-subcarriers are completely independent), the performance is the worst. This is because the channel differences within each group are large, and a single reference pilot cannot effectively represent other subcarriers. As α increases, the inter-subcarrier channel correlation becomes stronger, and the estimation performance of the correlation-based method gradually improves. When α is close to 1, the MSE curve decreases significantly. This indicates that under high correlation, the correlation-based method can well represent the channel of the entire group of subcarriers, and its estimation performance is close to that of the existing method. Thus, the correlation-based method is more suitable for application in channel environments with strong frequency-domain correlation, while its performance deteriorates significantly in scenarios with severe frequency-selective fading.

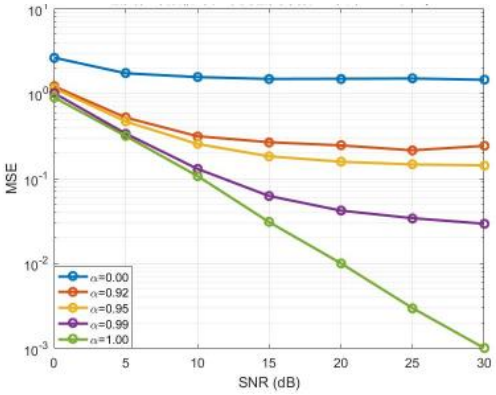

Fig. 8. MSE curves of relevant methods under different correlation coefficients.

D. System Bit Error Rate (BER) Performance Analysis

As shown in Fig. 9, with the improvement of signal-to-noise ratio (SNR), the bit error rate (BER) of both the existing method and the correlation-based method decreases. The overall trend in the figure is that as SNR increases, the BER of both methods decreases exponentially. That is, the bit error rate decreases significantly when channel quality improves. Among them, the BER curves of the two methods almost coincide with only slight differences. The local enlarged view shows the region of 20-25 dB, where four curves are very close. Overall, the BER performance of the two methods is very similar. This is because the channel conditions are relatively flat and the correlation of subcarriers is adopted, so the performance of the existing method and the correlation-based method is quite similar.

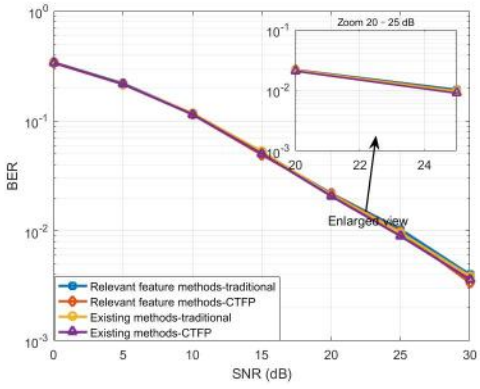

Fig. 9. Comparison of BER performance in the GFDM system.

V. Discussion

The channel estimation method for GFDM systems based on correlation characteristics is mainly suitable for the EPA (Extended Pedestrian A) channel model. This model corresponds to indoor communication scenarios with low speed or static terminals and has strong practical and engineering significance. For example, in typical application scenarios such as the Internet of Things and smart home systems, multiple indoor communication terminals access the same local area network at the same time, where the geographic locations of these terminals are close to each other. These terminals are usually static or move at a low speed, and their channels show strong correlation in the time, frequency, and spatial domains. Existing channel estimation methods based on correlation characteristics and pilot reduction mainly rely on the assumption of frequency domain correlation. Compared with these methods, the proposed method further considers practical application scenarios and introduces spatial correlation on the basis of frequency domain correlation. As a result, the proposed method can improve channel estimation performance and reduce pilot overhead in specific scenarios. Fig. 10 shows the practical application scenario of a channel estimation method for GFDM systems based on correlation and CTFP pilots.

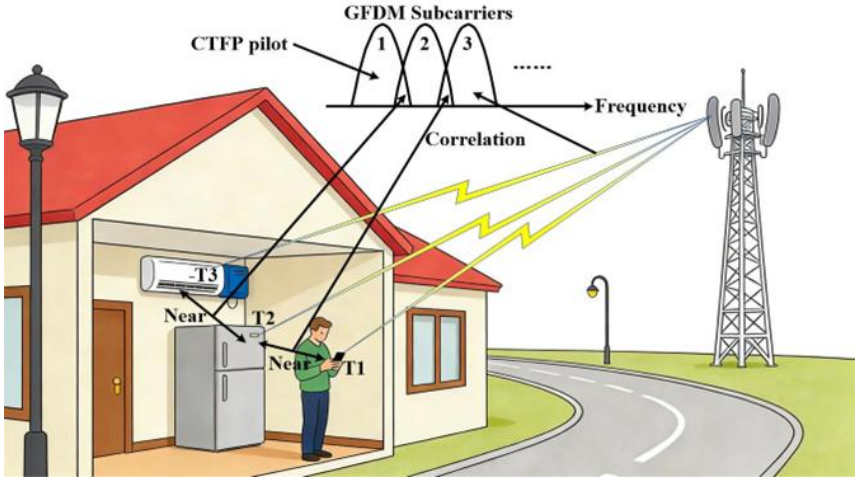

Fig. 10. Practical application scenario of a channel estimation method for GFDM systems based on correlation and CTFP pilots.

However, the GFDM channel estimation method based on correlation characteristics also has certain limitations. This method strongly depends on the correlation of terminals in the frequency and spatial domains. Therefore, in channel environments that are wide, where terminals are sparsely distributed and channel correlation is weak, the performance of this method will significantly degrade, and it may even become unsuitable. In addition, in high mobility scenarios targeted by Orthogonal Time Frequency and Space (OTFS) systems, the time variation of the channel becomes much stronger. In such cases, the correlation assumption is difficult to satisfy, and this type of channel estimation method cannot be effectively applied.

VI. Conclusion

Traditional channel estimation methods for GFDM systems rely on adding more pilot sequences, thus reducing the information transmission rate. To address the above problem, a correlation-based channel estimation method is proposed, and a two-dimensional block pilot sequence based on time domain and frequency domain is designed. This method utilizes the correlation between subcarriers, thus reducing the time slot overhead of pilot resources. Simulation results show that under the premise of the same total time overhead, the mean square error (MSE) and bit error rate (BER) performance of the proposed correlation-based channel estimation method are basically consistent with those of the existing method. However, the information transmission performance is improved by about 14.97% compared with the existing method when the time slot width is 0.096 ms, about 10.74% when the time slot width is 0.128 ms, and about 2.59% when the time slot width is 0.48 ms. This result indicates that when the system is sensitive to time-slot resources, the channel estimation method based on correlation can significantly improve transmission efficiency. It is particularly advantageous in high-density multi-carrier communication scenarios. Simulation experiments verify the reliability of the above method. This research result can provide theoretical support for the design and implementation of GFDM transmission systems in the future. The pilot structure of the correlation-based channel estimation method exhibits better channel estimation performance when the correlation between adjacent subcarriers is strong. In the future, further research is needed to study accurate channel estimation methods when the correlation is weak. This method has potential application value in future GFDM systems, as well as in new multi-carrier wireless communication systems such as 5G and 6G. Its low pilot overhead and high transmission efficiency make it suitable for various scenarios, including the Internet of Things, large-scale MIMO, vehicular networks, and low-latency communications. By further optimizing the pilot design and channel estimation algorithm, it is possible to achieve higher data throughput and better spectrum utilization while maintaining system robustness.

Acknowledgment

The research was funded by National Natural Science Foundation of China (NSFC):62441401.

REFERENCES

[1] Hamid E Y. DFT-based channel estimation for GFDM on multipath channels[C]//2018 10th International Conference on Information Technology and Electrical Engineering (ICITEE). IEEE, 31-35, 2018. DOI: 10.1109/ICITEED.2018.8534919.

[2] Tazehkand B M, Aghdam M R G, Abdolee R, et al. Optimal prototype filter design in GFDM systems for self-interference elimination: A novel signal processing approach[J]. Signal Processing, 2025, 227: 109711, 2025. DOI:10.1016/j.sigpro.2024.109711.

[3] Shayanfar H, Zhu W P, Swamy M N S. Compressed sensing based channel estimation for GFDM systems in high mobility scenario[C]//2023 IEEE 24th International Workshop on Signal Processing Advances in Wireless Communications (SPAWC). IEEE,266-270, 2023. DOI: 10.1109/SPAWC53906.2023.10304479.

[4] Fettweis G, Krondorf M, Bittner S. GFDM-generalized frequency division multiplexing[C]//VTC Spring 2009-IEEE 69th Vehicular Technology Conference. IEEE,1-4, 2009. DOI: 10.1109/VETECS.2009.5073571.

[5] Tazehkand B M, Aghdam M R G, Vakilian V, et al. Novel successive interference cancellation (SIC) with low-complexity for GFDM systems[J]. IEEE Access, 10: 40063-40072, 2022. DOI: 10.1109/ACCESS.2022.3167051.

[6] Vincent V, Hamid E Y, Permana A K. Adaptive threshold for discrete fourier transform-based channel estimation in generalized frequency division multiplexing system[J]. ETRI Journal, 46(3): 392-403, 2024. DOI:10.4218/etrij.2023-0003.

[7] Tai C L, Su B, Jia C. Interference-precancelled pilot design for LMMSE channel estimation of GFDM[C]//2020 IEEE 21st International Workshop on Signal Processing Advances in Wireless Communications (SPAWC). IEEE,1-5, 2020. DOI: 10.1109/SPAWC48557.2020.9154242.

[8] Na Z, Pan Z, Xiong M, et al. Turbo receiver channel estimation for GFDM-based cognitive radio networks[J]. IEEE Access, 6: 9926-9935, 2018. DOI: 10.1109/ACCESS.2018.2803742.

[9] Zhang W, Zhang Z, Qi L, et al. Lattice-reduction-aided signal detection in spatial multiplexing MIMO–GFDM systems[J]. Physical Communication, 33: 71-77, 2019. DOI:10.1016/j.phycom.2018.12.015.

[10] Ehsanfar S, Matthé M, Zhang D, et al. Interference-free pilots insertion for MIMO-GFDM channel estimation[C]//2017 IEEE Wireless Communications and Networking Conference (WCNC). IEEE, 1-6, 2017. DOI: 10.1109/WCNC.2017.7925957.

[11] Bello A M, Suwansantisuk W, Song I, et al. Joint synchronization and channel estimation for GFDM systems[J]. IEEE Access, 2024. DOI: 10.1109/ACCESS.2024.3457030.

[12] Mohammadian A, Tellambura C. Joint channel and phase noise estimation and data detection for GFDM[J]. IEEE Open Journal of the Communications Society, 2: 915-933, 2021. DOI: 10.1109/OJCOMS.2021.3073348.

[13] Liu Y, Zhu X, Lim E G, et al. Robust semi-blind estimation of channel and CFO for GFDM systems[C]//ICC 2019-2019 IEEE International Conference on Communications (ICC). IEEE, 1-7, 2019. DOI: 10.1109/ICC.2019.8761213.

[14] Inga J, Peñafiel B, Ortega A. Pilot Channel Estimation for Improve the Non-Linear Effects on GFDM-MIMO Scheme[C]//International Conference on Science, Technology and Innovation for Society. Cham: Springer Nature Switzerland, 12-24, 2024. DOI: 10.1007/978-3-031-87065-1_2.

[15] Wang M, Chen X, Yuan B. A CFO Estimation Method Based on Preamble Symbols for GFDM[C]//2022 5th International Conference on Communication Engineering and Technology (ICCET). IEEE, 90-94, 2022. DOI: 10.1109/ICCET55794.2022.00026.

[16] Jeong J, Park Y, Weon S, et al. Eigendecomposition-based GFDM for interference-free data transmission and pilot insertion for channel estimation[J]. IEEE Transactions on Wireless Communications, 17(10): 6931-6943, 2018. DOI: 10.1109/TWC.2018.2864995.

[17] Shayanfar H, Saeedi-Sourck H, Farhang A. CFO and channel estimation techniques for GFDM[C]//2018 IEEE MTT-S International Microwave Workshop Series on 5G Hardware and System Technologies (IMWS-5G). IEEE, 1-3, 2018. DOI: 10.1109/IMWS-5G.2018.8484326.

[18] Ehsanfar S, Matthé M, Zhang D, et al. Theoretical analysis and CRLB evaluation for pilot-aided channel estimation in GFDM[C]//2016 IEEE Global Communications Conference (GLOBECOM). IEEE, 1-7, 2016. DOI: 10.1109/GLOCOM.2016.7842323.

[19] Anish Pon Yamini K, Akhila S V, Suthendran K, et al. Analysis of channel estimation in GFDM system[M]//Data Engineering and Communication Technology: Proceedings of ICDECT 2020. Singapore: Springer Singapore, 679-687, 2021. DOI: 10.1007/978-981-16-0081-4_68.